Contents — E through G

ANTARCTIC ANALOGUES FOR MARS EXPLORATION: A RAMAN SPECTROSCOPIC STUDY OF BIOGEOLOGICAL SIGNATURES.

Howell G..M. Edwards[1], Caroline A. Moody , Susana E. Jorge Villar[1,2] and the late David D. Wynn-Williams[3]

[1] Department of Chemical and Forensic Sciences, University of Bradford, Bradford BD7 1DP, UK.
e-mail: h.g.m.edwards@bradford.ac.uk

[2] Area de Geodinamica Interna, Facultad de Humanidades y Educacion, University of Burgos, Calle Villadiego S/N, 09001 Burgos, Spain.

[3] Antarctic Astrobiology , British Antarctic Survey , High Cross , Madingley Road , Cambridge CB3 0ET , UK.

Introduction: The present conditions at the surface of Mars are not conducive to the survival of life forms, with the thin atmosphere, lack of water, a highly-oxidising regolith and significant UV insolation. The Antarctic provides a terrestrial model with a transect from the maritime, where epilithic colonies can survive through the production of protectant biochemicals, to endolithic systems at the "limits of life" where existence at the surface is impossible [1,2] . In the Antarctic Dry Valleys, the extremely low humidity coupled with low temperatures reaching - 35°C, strong katabatic winds blowing from the Polar plateau and intense UV-radiation exacerbated by atmospheric ozone depletion at higher latitudes provides a putative analogue for the hostile conditions that life must tolerate for survival at or near the Martian surface [3,4].

This extreme terrestrial ecosystem is believed to mirror the conditions under which the evolution of organisms would have had to adapt to the steadily worsening environmental situation on Mars , as exemplified by Epochs III and IV , which effectively describe the Martian surface , subsurface and atmosphere over the last 1.5 million years [4 ,5].]The surface temperatures on Mars range from –123 ^{0}C to + 25 ^{0}C, it's atmosphere is thin and transmits UVB and UVC radiation , and the presence of liquid water at the planetary surface is still conjectural. Clearly , the identification of Antarctic microniches which are amenable to analytical study can provide suitable examples of extremophile terrestrial behaviour of direct relevance to Mars.

Antarctic extremophiles : Special strategies are vital for the adaptation of Antarctic lichens and cyanobacteria to these extreme conditions [6,7]; in addition, the Antarctic provides a gradual change in ecosystem tolerance along a transect from the relatively milder maritime conditions experienced at the coast through to the cryptoendoliths , which are effectively the most adaptable colonies in the Polar region, after which only fossil cyanobacterial evidence is found at the highest latitudes [8,9]. This means that the different strategies being enforced for the survival of these organisms under worsening environmental habitats can be exploredexperimentally and evaluated analytically to assist the predictions of response of organisms to extremes of stress.

To reduce the amount of UVB and UVC radiation reaching the organisms , it is essential that the colonies produce a suite of radiation-protective chemicals for filtering out the low-wavelengths whilst still maintaining their capability for accessing the photosynthetically active wavelengths required for their metabolic processes [10,11]. Hence, it is possible to identify as protective biomolecules complex organic chemicals such as beta-carotene and a range of pigments such as parietin , rhizocarpic acid and calycin --- the former is believed to act as a UV –filter and also function in a DNA-repair mechanism for cell damage caused through radiation exposure, whilst the latter pigments are thought to behave as accessory radiation protectants [11,12,13] . We have carried out some experiments over a two-year period on Antarctic colonies which have been subjected to full radiation exposure at Jane Col , Leonie Island , compared with other colonies at the same site which have been shielded by UVB- and UVC–absorbent plastic cloches. Using nondestructive Raman techniques, it is possible to monitor the production of pigments in response to changes in the environmental situation---in particular , the relative proportions of parietin and beta-carotene in protected and unprotected colonies indicates a possible dualistic role for these pigments [14,15].

The production of hydrated calcium oxalates by colonies under stress is also a key factor of change in other circumstances ; it has been suggested that these oxalates are produced as chelators of heavy metals in the substrate, as water storage devices , acidity controllers and as anti-herbivoral agents. We have recently found evidence for the biogeological modification of iron oxides by extremophilic colonies in the most highly stressed conditions . The importance of this is two-fold , since it not only provides another parameter of knowledge for the understanding of the mechanisms by which terrestrial organisms survive these extremes , but it also gives a clue as to the sort of biogeological changes that have been effected by extremophilic organisms at the limits of life. Hence, in a situation , such as that which probably applied on Mars , any vestiges of extremophilic life would be incapable of tolerating or adapting to the worsening conditions, and they would pass into the fossil record. The clues to their former existence would then be totally found in the geological record and in a suite of unusual relict chemical compounds found there.

Raman spectroscopy : The viability of Raman spectroscopy to identify the key spectral biomarkers of extinct or extant life in the biogeological record has been amply demonstrated for the analysis of Antarctic endoliths [16,17] . The Raman biosignatures of key protectant molecules have been established for the identification of the strategies adopted by cyanobacteria for the colonisation of geological strata . An important requirement here is the ability of the analytical spectroscopic tecnique employed to locate and identify the key biomarkers in the geological systems that might be expected to be encountered in planetary exploration.

The miniaturisation of laboratory-based Raman spectrometers to a size which makes them suitable for part of an instrumentation suite on a robotic lander on a planetary surface has been receiving much attention recently [17-19]. Clearly, the evaluation of prototype instruments for Martian surface or subsurface exploration would be well served by analytical experiments involving Antarctic materials.

In this paper we shall discuss the comparative data obtained from several Raman instruments on Antarctic extremophiles which will include an epilith from Signy Island, a chasmolith from the Lake Hoare LTER site in the Dry Valleys , a cyanobacterial mat from Lake Vanda and an endolith from Mars Oasis (this latter specimen must be considered to be especially relevant to planet Mars !). Some of the advantages of the Raman technique for adoption as analytical instrumentation on a mission to Mars will emerge from this study.

In particular , the capability of the Raman technique for the identification of the spectral biomarkers under different conditions , without special sample preparation and in a micro-sampling mode , giving a specimen "footprint" of only several microns diameter is assessed . A critical factor in this series of experiments is the wavelength selection of the laser excitation employed for the analysis and information from spectra recorded with visible and near-infrared laser sources [20] . This information is relevant for the design of miniaturised Raman instruments that will have the objective of searching for extant or extinct life on planetary surfaces or subsurfaces, especially Mars.

References : [1] Wynn-Williams D.D. et al. (2000) *Biblio. Lichenologica ,75 ,*275-288 . [2] Wynn-Williams D.D. (2000), in *The Ecology of Cyanobacteria : Their Diversity in Time and Space* ,eds. Whitton B.A. , Potts M. , Kluwer, Dordrecht , 341-366 . [3] Wynn-Williams D.D. et al. (2001),in *Proc 1st Euro. Workshop on Exo-Astrobiology, Frascati, May 2000*, eds. Ehrenfreund P. et al., ESA SP 496,225-237 . [4] Wynn-Williams D.D. , Edwards H.G.M. (2000) *Icarus , 144,* 485-503 . [5] McKay C.P. (1997) *Origins Life Evol. Biosphere , 27 ,* 263-289 . [6] Siebert J. et al. (1996 *) Biodiversity Conserv. , 5 ,*1337-1363 . [7] Kappen L. (1993) , in *Antarctic Microbiology ,* ed. Friedmann E.I. , Wiley-Liss , New York , 433-490 . [8] Friedmann E.I. (1982) *Science , 215 ,*1045-1053 . [9] Friedmann E.I. et al. (1988) *Polarforschung , 58 ,* 251-259 . [10] Nienow J.A. et al. (1988) *Microbial Ecology , 16 ,* 271-289 . [11] Cockell C.S. , Knowland J. (1999) *Biol. Revs. Camb. Phil. Soc. , 74 ,*311-345 . [12] Vincent W.F. et al. (1993) *J. Phycology , 29 ,* 745-755 . [13] Wynn-Williams D.D. et al. (1999) *Euro. J. Phycology , 34 ,* 381-391 . [14] Holder J.M. et al. (2000) *New Phytologist , 145 ,* 271-280 . [15] Edwards H.G.M. et al. (1998) *Soil Biol. Biochem., 30 ,* 1947-1953 . [16] Russell N.C. et al. (1998) *Antarctic Sci., 10 ,* 63-73 . [17] Edwards H.G.M. et al. (1999) *,* in *The Search for Life on Mars* , ed Hiscox J.A. , British Interplanetary Soc. , London , 83-88 . [18] Haskin L.A. et al. (1997) *JGR Planets , 102 ,* 19293-19306 . [19] Wang A. et al. (1999) *JGR ,104 ,*27067-27077 . [20] Edwards H.G.M. et al. (2003) *Intl. J. Astrobiology , 1 ,* 333-348 .

A MICROPHYSICALLY-BASED APPROACH TO INFERRING POROSITY, GRAIN SIZE, AND DUST ABUNDANCE IN THE SEASONAL CAPS FROM ATMOSPHERICALLY-CORRECTED TES SPECTRA.

J. Eluszkiewicz[1] and T. N. Titus[2], [1]Atmospheric and Environmental Research, Inc., 131 Hartwell Ave., Lexington, MA 02421, jel@aer.com, [2]U.S. Geological Survey, 2255 North Gemini Dr., Flagstaff, AZ 86001, ttitus@usgs.gov.

Introduction: One of the highlights of the TES observations in the polar regions has been the identification of a "cryptic" region in the south where CO_2 appears to be in the form of a solid slab rather than a fluffy frost [1]. While the exact mechanism(s) by which the cryptic region is formed are still subject of some debate, it appears certain that a type of rapid metamorphism related to the high volatility of CO_2 ice is involved. The high volatility of CO_2 ice under martian conditions has several Solar System analogs (N_2 on Triton and Pluto, SO_2 on Io), thus making the martian cryptic region somewhat less cryptic and certainly non-unique among planetary objects. In an end-member scenario, both the formation and the spectral properties of the cryptic region (and of other areas in the seasonal caps) can be quantitatively modeled by considering sintering of an ensemble of quasi-spherical CO_2 grains [2]. This model includes the special case of instanteneous slab formation, which occurs when the grains are sufficiently small (in the submicron range) so that their sintering timescale is short relative to the deposition timescale (a situation analogous to the "sintering" of water droplets falling into a pond).

Physics of Sintering: Originally, the idea of annealed slabs of CO_2 in the martian seasonal caps was proposed based on an analysis of densification timescales [2]. Recently, we have also evaluated the role played by the non-densifying sintering mechanism caused by vapor transport (Kelvin effect). The main conclusion from this recent work is that the seasonal CO_2 deposits on Mars rapidly metamorphose into an impermeable slab regardless of the initial grain size. The slab forming by this mechanism is expected to contain quasi-spherical voids that then undergo slow elimination by the densifying mechanisms. This densification process *is* strongly grain-size dependent, which can be used to explain the persistence of both low- and high-emissivity areas (e.g., the cryptic region and Mountains of Mitchell, respectively). The proposed texture for the martian CO_2 deposits is consistent with both TES and other observations (in particular, the porous texture of the slab is consistent with the mean density of the seasonal deposits inferred from the MOLA data being less than the theoretical density of solid CO_2 [3]) and it has important consequences for the modeling of the physical properties of the martian seasonal frost. Specifically, the radiative properties of the frost (e.g., albedo and emissivity) are more properly modeled by treating radiative transfer in a slab of solid CO_2 containing spherical voids (and other impurities such as dust grains) rather than by the usual model of spherical CO_2 and dust grains *in vacuo*. In the present study, this problem is tackled by finding the Mie solution for a spherical particle embedded in an absorbing host medium [4]. The Mie solution is then applied in a multiple scattering code [5] to compute the radiative properties of the martian CO_2 deposits.

Application of the New RT Model: The chief advantage of the new RT model is its connection to the microphysical model of the cap texture and, consequently, its predictive capability. In particular, the new model does not require the notion of meter-sized Mie boulders of solid CO_2 in order to explain the high emissivities in the cap spectra (e.g., in the cryptic region) but instead relates them to low porosity. The strong porosity dependence of the computed emissivity suggests that the density evolution obtained from the sintering model can be coupled with the radiative transfer calculations to predict the evolution of emissivities. Preliminary results presented at the 6th Mars Conference [6] have demonstrated the capability of the new model to mimic the observed evolution of the cap emissivity (represented as the depth of the TES 25-μm band, BD_{25}).

Modeling the Shape of TES Spectra: In addition to generating a semi-quantitative agreement with the evolution of BD_{25}, the new model is capable of providing a quantitative match to the shape of the TES spectra. For this more quantitative test, it is important to remove the component of the spectra related to atmospheric dust, which we accomplish using an approach based on the emission phase function (EPF) [7]. To date, 105 EPF-corrected spectra of the caps have been generated. An example of an EPF-corrected spectrum and the model spectra computed using the new RT model are shown in Figure 1. The refractive indices for solid CO_2 used in the calculations are as in [8], while the dusty spectra have been computed using optical constants for palagonite [9]. Application of the new model to match the TES spectra can in principle lead to maps of the porosity, void size, and dust content for the polar caps. In the example shown in Figure 1, a fairly good match to the observed spectrum is obtained for a slab containing 5-μm voids at 1% porosity with a

fractional abundance of 1-µm dust grains of 5 x 10^{-4} by volume (the presence of dust is responsible for the shift of the frequency of mimimum emissivity longward of 25 µm). Of course, the RT solution for these parameters is non-unique, and this will necessitate the development of a maximum-likehood inversion method utilizing *a priori* information. The results from the sintering model might in fact be used as an *a priori* constraint (i.e., in a given location, the solution for porosity at different times should be consistent with the porosity evolution predicted by the sintering model). In addition, several important factors neglected so far (e.g., variable cap thickness, nonuniform density distribution with depth, presence of a thermal gradient) should be included, some of which could further improve the agreement between the coupled microphysical/radiative transfer model and TES observations. Ultimately, the new model will provide a powerful observationally-based tool for the modeling of the coupled surface-atmosphere system on Mars.

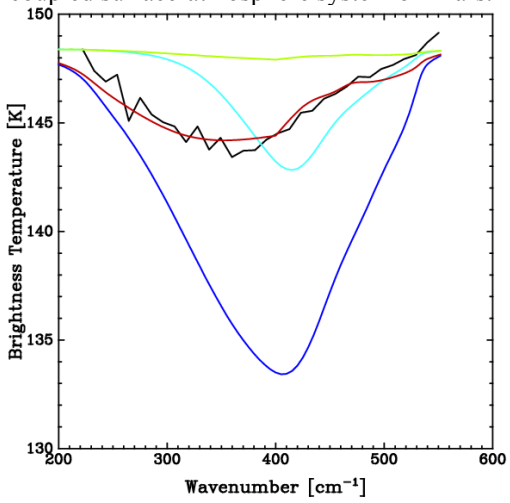

Figure 1: Black line: Observed spectrum. Dark blue line: computed spectrum with 5-µm voids, no dust. Light blue line: computed spectrum with 1-µm voids, no dust. Green line: Computed spectrum with 1-µm voids, 5 x 10^{-4} by volume of dust. Red line: Computed spectrum with 5-µm voids, 5 x 10^{-4} by volume of dust. All computed spectra assume a kinetic temperature of 146 K, slab thickness of 1 meter, 1% porosity, and dust grain size of 1 µm.

Acknowledgement: One of the authors (JE) has been funded by the Mars Data Analysis Program.

References: [1] Kieffer H. et al. (2000) *JGR 105,* 9653. [2] Eluszkiewicz J. (1993) *Icarus 103,* 43. [3] [3] Smith D. E. et al. (2001) *Science 294,* 2141. [4] Yang P. et al. (2002) *Appl. Opt. 41,* 2740. [5] Stamnes K. et al. (1988) *Appl. Opt. 27,* 2502. [6] Eluszkiewicz J. and T. N. Titus (2003) 6th Mars Conference (www.lpi.usra.edu/meetings/sixthmars2003/pdf/3046.pdf). [7] Titus T. N. and H. H. Kieffer (2001) 33rd DPS Meeting. [8] Hansen G. B. (1997) *JGR 102,* 21,569. [9] Roush T. et al. (1991) *Icarus 94,* 191.

THE ABILITY TO PROBE THE MARTIAN POLAR SUBSURFACE VIA GROUND-PENETRATING RADAR. W. M. Farrell and P. R. Mahaffy, NASA/Goddard Space Flight Center, Greenbelt MD 20771, William.Farrell@gsfc.nasa.gov, Paul.R.Mahaffy@gsfc.nasa.gov

Introduction: Ground-penetrating radar (GPR) offers the exciting possibility of remote sensing below the Martian surface for trapped aquifers. A GPR is currently heading to Mars onboard Mars Express (MEX) and a GPR is in consideration to be onboard Mars Reconnaissance Orbiter (MRO) in 2005. While such orbital systems offer great potential for polar stratigraphy studies, their ability to penetrate deep into the Martian polar ice is a function of both the intervening ionospheric density and the overlying ground ice conductivity. The influence of both signal-altering layers will be discussed.

Polar Ice and Water: Clifford[1,2] has suggested that the trapped basal lakes may form at the bottom of the polar cap, along the ice/regolith interface. Such deep aquifers form either due to insulation effects from the overlying ice, local geothermal hot spots, or frictional heating from glacial sliding. Chasma Boreale and Australe have been suggested to be of possible fluvial origin[3], formed by discharging from a past-trapped aquifer within the cap. Basal lakes and deep ice cap melting may ultimately feed a deeper water table that ultimately supplies the cryosphere at lower latitudes[2]. Evidence for this areal extended ice cryosphere has recently been obtained by the GRS experiment onboard Mars Odyssey[4,5]. Similar basal lakes have been found in Antarctica and allegorical discharging lakes are found in Iceland[1,2].

GPR Signal Propagation: In order for orbiting GPR's to examine the polar subsurface for trapped aquifers, their radio signal must first propagate through the attenuating ionosphere. The operating frequency for the MEX/Mars Advanced Radar for Subsurface and Ionospheric Sounding (MARSIS) is 1-5 MHz with a transmitting power of 15 W. The ionospheric plasma frequency, fp, the blocking frequency below which the ionosphere is opaque, extends from about 3 MHz on the dayside of Mars but quickly drops to about ~300 kHz just past (about 10^o from) the terminator. Hence, to minimize the effect of the ionosphere, sounding the polar subsurface from orbit should occur when the overlying polar ionosphere is not illuminated by the sun. Ideal observation periods for MARSIS nighttime polar sounding will be displayed in the presentation.

Besides the ionosphere, the overlying polar ice over a basal lake also attenuates GPR signals. It is demonstrated that the ability of the MARSIS 15 W transmitter to yield a detectable return signal (above the cosmic background level) from an aquifer located at depth, d, varies as $d \sim k\ \sigma^{-1}$, where k is 0.01 S, for a MEX altitudes of 800 km and a transmission frequency of 4 MHz. Consequently, if the polar ice has a consistency comparable to freshwater ice, with $\sigma \sim 10^{-3}$ S/m, a return signal from an aquifer is possible only in the first few meters of the cap. For depths > 10 m, the ice attenuates the signal (both incoming and outgoing) to the extent that the reflected pulse cannot return to the receiver at strengths above the ambient background noise. In contrast, if the cap consistency is more like firm snow, with $\sigma \sim 10^{-5}$ S/m, aquifer detection with a return signal above the noise level is possible to a depth of about 1 km. Clearly, the as-yet-determined character and consistency of the overlying ice will have a significant impact on the successful detection of a polar aquifer.

Future Concepts: There have been other proposed strategies for sounding the polar subsurface. During last year's Scout Mission Opportunity, a multi-institutional team proposed the Mars-POLAR Montgolfier balloon mission to perform a 30-60 day overflight of the north polar region at 4 km altitude. Included in the payload was a 3W Radio Beacon Sounder (RBS) that had the following advantages over their orbital counterparts:

-Proximity to the source by a factor of 100 increases the delivered signal strength to the ground by 30 dB compared to orbital instruments.

-Platform below the shielding, contaminating, and attenuating effects of the ionosphere.

-Ease in deployment of large antenna via direct integration into the balloon, thereby reducing deployment mass and risks that plague orbital sounder antenna deployments.

The feasibility of aquifer detection for a balloon-based system will be compared and contrasted to its orbital counterpart.

References: [1] Clifford, S.M. (1987) *JGR, 92,* 9135. [2] Clifford, S. M. (1993) *JGR, 98,* 10973. [3] Anguita F. et al. (2000) *Icarus, 144,* 302. [4] Mitrofanov, I., et al. (2002), *Science, 297,* 78. [5] Feldman, W. C., et al., *Science, 297,*75.

Association of Measured Distribution of Near-Surface Hydrogen at High Northerly Latitudes with Surface Features on Mars. W.C. Feldman[1], S. Maurice[2], T.H. Prettyman[1], M. T. Mellon[3], S.W. Squyres[4], S. Karunatillake[4], R.C. Elphic[1], H.O. Funsten[1], D.J. Lawrence[1], and R.L. Tokar[1], [1]Los Alamos National Laboratory, Los Alamos, New Mexico, [2] Observatoire Midi-Pyrenees, Toulouse, France, [3] LASP, University of Colorado, Boulder, CO, [4]Cornell University, Ithaca, NY

Introduction: Lower-limit estimates of the global abundance of hydrogen on Mars reveal a remarkable surface distribution [1]. Three discrete reservoirs are apparent. Two of the reservoirs fill large areas that cover much of the northern and southern high-latitude regions, and the third has several components at equatorial to mid latitudes. A map of water-equivalent hydrogen, M_{H2O}, north of +50° latitude derived from epithermal-neutron counting rates measured between areocentric longitudes of 100° and 181° (when the seasonal CO_2 frost cover was completely absent) [1], is shown in Figure 1. M_{H2O} is seen to maximize at 100% by mass, at the north-polar residual cap. This maximum is a component of a generally water-rich region that covers much of the surrounding high-latitude terrain. This region has a local minimum that overlies Olympia Planitia, a secondary maximum that follows a narrow arc at about +75° latitude that connects 100° to 180° east longitude, and a pronounced secondary maximum that is centered at about +70° latitude and –135° east longitude. Whereas the arc-shaped maximum overlies a similar arc of surface water ice that is apparent in visible images of Mars, the secondary maximum has no apparent surface feature. Another feature of the enhanced reservoir of hydrogen at high northerly latitudes is that it is pinched off on one side by a relatively low H_2O-abundance region that is centered on –45° longitude.

Intercomparison with Surface Features: In an attempt to search for physical properties of the Martian surface that are associated with the foregoing hydrogen abundance features, we overlayed contours of M_{H2O} onto maps of thermal inertia, albedo, and rock abundance [2,3,4]. Starting first with the albedo (shown in Fig. 2), we see that the highest albedo, which corresponds to surface water-ice deposits, overlies the central maximum in M_{H2O} and the outlying arc of high M_{H2O}. Additionally, the secondary maximum in M_{H2O} lies within an extended region of relatively high albedo. An extended region of low albedo that is centered on –45° longitude at the mouth of Chasma Boreale, is coincident with the pinched-off portion of the

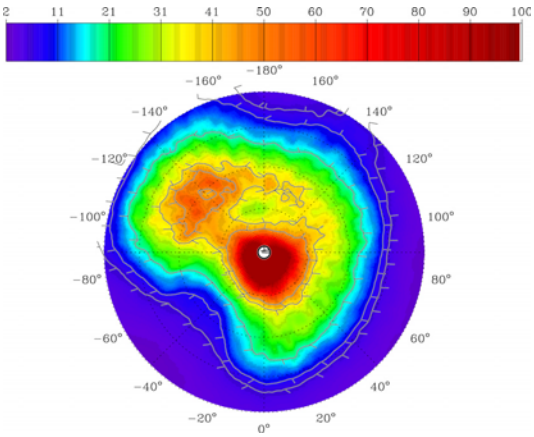

Fig. 1. Map of lower-limit abundances of M_{H2O}, shown in orthographic projection north of +50° latitude. The contours correspond to 7%, 10%, 20%, 40% and 50% M_{H2O}, progressing inward from the outside.

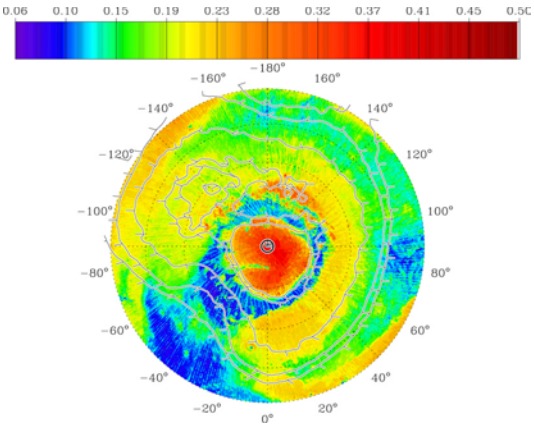

Fig. 2. Map of albedo shown in orthographic projection north of +50° latitude. Contours of mass % H_2O are the same as in Fig. 1.

high-latitude, high M_{H2O} terrain. Extension of this region to lower latitudes is shown in Fig. 3, which intercompares M_{H2O} with rock abundance and albedo. Inspection shows that most regions of high rock abundance and low albedo overlie regions of relatively low M_{H2O}. However, the inverse is not true. There are regions of low rock abundance (and high albedo) that are coincident with regions of low M_{H2O}. In addition, there is a region just south of Arabia Terra, and between

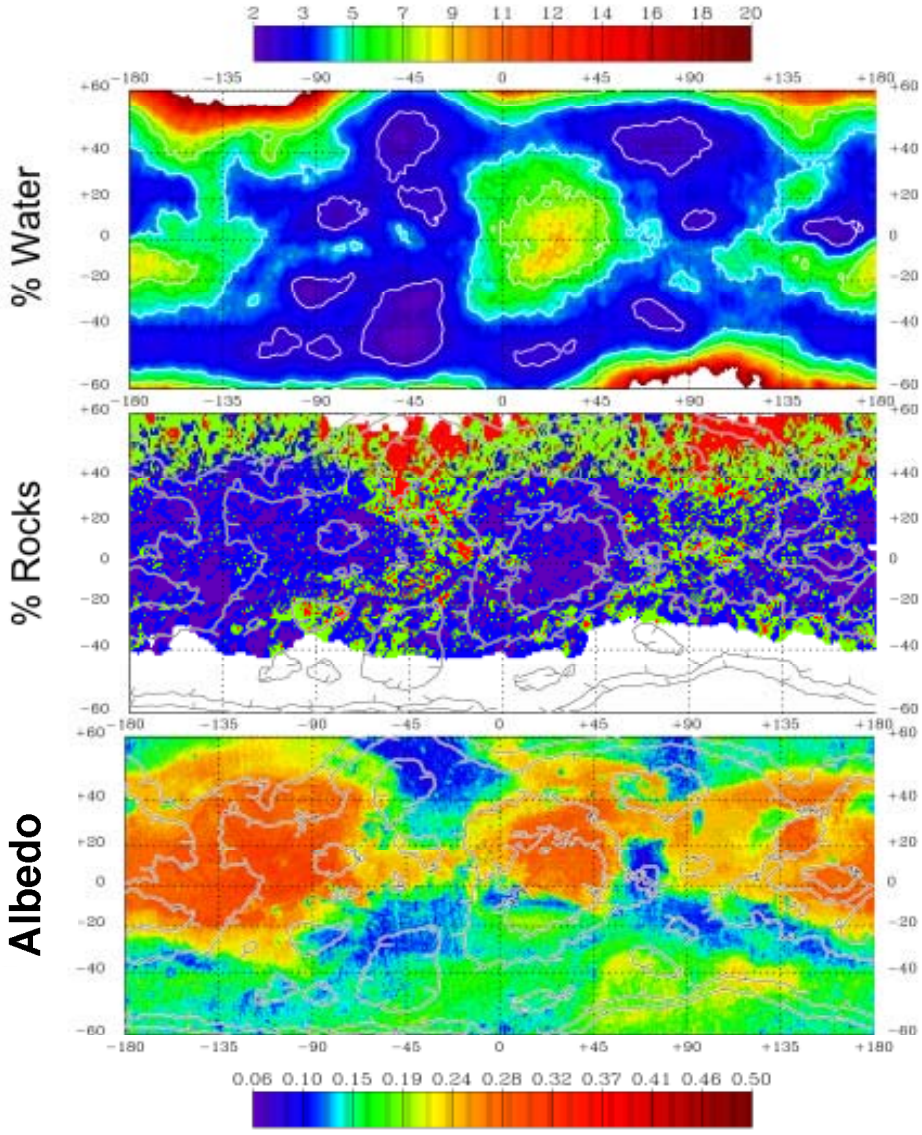

Fig. 3. Maps of M_{H2O}, percent abundance of rocks [4], and albedo [2,3] all in cylindrical projection between ±60°. Contours of M_{H2O} corresponding to 3%, 5%, and 7% are overlayed on all three maps. The colors in the middle panel correspond to 0%-5% [purple], 5%-10% [blue], 10%-17% [green], and >17% [red] rock abundance, respectively.

–20° and –40° latitude near 180° east longitude where the albedo is not high, the rock abundance is low, and M_{H2O} is relatively high. Altogether, these associations suggest that no single process can explain all of the observed structure of enhanced M_{H2O} deposits on Mars. For example, contributing factors could be the physical structure of subsurface soils (such as porosity and permeability), the mineral and chemical composition of these soils, the time dependence of the partial pressure of water vapor in the atmosphere, and the time-dependence of, and insulating properties of the overlying dust cover.

References: **[1]** Feldman, W.C., et al., J.G.R., submitted, 2003, [2] Mellon, M.T., et al., LPSC, XXXIII, Houston, TX, 2002, [3] Christensen, P.R., et al., J. G.R., 106, 23823-23871, 2001, [4] Christensen, P.R., Icarus, 68, 217-238, 1986.

AMAZONIAN GEOLOGIC HISTORY OF THE NORTH POLAR CAP OF MARS: STRATIGRAPHY, MELTING, AND RETREAT Kathryn E. Fishbaugh[1] and James W. Head III[1], [1]Brown University, Dept. Geol. Sci., Box 1846, Providence, RI 02912, kathryn_fishbaugh@brown.edu, james_head_III@brown.edu

Introduction: Mariner 9 [1,2] and Viking era studies [e.g., 3] showed the polar caps to consist of layers with varying amounts of dust and ice, termed the polar layered deposits (Apl), and a residual polar cap (Api) consisting of ice and dust overlying these [4]. In the north, this residual cap consists of water ice and in the south of water and CO_2 ice [4], yet CO_2 clathrate may also compose a percentage of the Apl and residual ice at both poles [5]. Most authors believe that the variability in dust content within the Apl is to some degree controlled by orbital oscillations [6-8]. Only recently have researchers considered the martian polar caps as possibly behaving similarly to terrestrial ice caps, both glaciologically and geologically. *Tanaka and Kolb* [9] and *Kolb and Tanaka* [10] have outlined a possible geologic history of the poles, suggesting that melting and flow have not occurred. Yet, several authors have estimated ice flow rates, of mm to meters/yr [11-13], and Fisher [14] has put forth the idea that ice flow may play a crucial role in the forming of the northern spiraling troughs. Just as terrestrial ice sheets experience meltwater outbursts in the form of jökulhlaups, Chasma Boreale may also have been formed in part by melting of the Apl (possibly due to volcanic eruption) and outflow [15-17]. There is also geologic evidence for at least one stage of retreat of the north polar cap [18,19]. Thus, the martian north polar cap has a much more complex and Earth-like history than simple accumulation of residual ice and dust.

A major outstanding question in the study of the north polar cap is, "When did all of this occur?". *Tanaka and Scott* [4] have placed the beginning of Apl deposition for both caps in the Late Amazonian, and *Herkenhoff and Plaut* [20], based on crater counts, have estimated maximum surface ages of 7-15 x 10^6 yrs. (south) and <100 x 10^3 yrs. (north). The goal of our research thus far has been to piece together a possible history of the north polar cap from the end of Vastitas Borealis Formation (VBF) deposition in the Late Hesperian to the current estimates of the beginning of Apl deposition nearly 3 billion years later in the Late Amazonian. Thus, we have studied the major stratigraphy of the polar deposits, the evidence for growth and retreat of the polar cap, and its melting history.

Stratigraphy: As described above, the polar cap consists of two major units: the polar layered deposits (Apl) and the residual ice (Api) overlying these. *Howard et al.* [21] have described the stratigraphy of the Apl in detail using Viking data. The darker, dustier layers are laterally continuous and contain an unknown percentage of dust. Layer thicknesses vary; Viking images revealed major layers on the order of 5-25 m thick, while MOC has shown layer thicknesses down to the limit of resolution (~2 m) [22,23]. Recently, a darker, layered unit has been found to lie beneath the Apl [22,10,24,25]; *Tanaka et al.* [26] term this unit "polar layered deposits 1" (Apl_1) and give it an Early Amazonian age. We have referred to this unit as the basal unit. Building upon these previous studies of the basal unit, we have continued to investigate its major characteristics [27].

The basal unit consists of alternating light and dark layers. The darker layers are much thicker (10s of meters) and less easily eroded than the thinner ones which may consist of the ubiquitous planetary dust. Steep slopes (some near 40°) indicate possible cementation by water ice. Individual layers also erode at different rates, and some of the lower layers show evidence of eolian erosion. Since the basal unit is exposed in troughs within Olympia Planitia, the sublimation and wind erosion which produced the trough [28] is able to erode the basal unit as well. This erosion has left behind pits, ridges, residual mesas, and yardang-like forms.

The close geographical association of basal unit outcrops with the northern dunes suggests that the basal unit is probably the source for these dunes [24], just as *Thomas and Weitz* [29] found that the lower Apl was probably the dune source (before the basal unit was discovered). The Apl also appear to unconformably overlie the basal unit since the basal unit layers pinch-out along the contact, indicating that major erosion may have taken place between the end of basal unit deposition and the beginning of Apl deposition. It is also possible that deposition of the basal unit occurred in irregular patches, rather than in continuous layers, creating the illusion of an unconformity. Dark lenses found within the lower Apl layers may be dunes which eroded from the basal unit and migrated onto the young, still-forming Apl.

The best exposures of the basal unit lie within the troughs bordering and extending into Olympia Planitia and within the arcuate scarps at the head of Chasma Boreale. At its thickest point, the basal unit is approximately 400 m thick (1100 m, including Olympia Planitia) and pinches out somewhere near Chasma Boreale. According to *Byrne and Murray* [24], Olympia Planitia consists wholly of the basal unit.

We have investigated several theories of formation of the basal unit [30], including 1) eolian deposit, 2) outflow channel/oceanic deposit, 3) incorporation into basal ice, and 4) a remnant of several stages of polar cap retreat, and find that the latter scenario is most likely. Formation of the basal unit accounts for some of the Amazonian history of the north polar cap.

Melting of the Polar Cap: Using Viking data, two different theories on the formation of Chasma Boreale have arisen: katabatic wind erosion and sublimation [28] and melting and outflow [15,16]. We have examined these and formation by glacial flow and ablation using primarily MOLA data and find that the most likely mechanism of formation is a combination of sublimation, katabatic wind erosion, melting, and outflow [17]. The cause of such melting is still unknown but candidate triggers include: 1) volcanic eruption, 2) climate change of a scale large enough to cause melting, 3) incorporation of salts into the

lower layers, and 4) pressure melting due to the presence of a thicker cap. The basal unit may have played a crucial role in the creation of Chasma Boreale as it may have affected placement of water reservoirs and transportation of that water. In addition, much of the basal unit has been eroded by formation of Chasma Boreale; the floor and lobate deposits at the mouth may consist of modified lower layers of the basal unit. If the north polar cap underwent at least one stage of relatively large-scale melting, then this may have contributed in part to polar cap retreat.

Retreat of the North Polar Cap: We have described geologic evidence for at least one stage of polar cap retreat [19,31]. Unusual, rough, knobby depressions south of Olympia Planitia resemble kame-and-kettle topography, formed on Earth by the deposition of englacial sediment and melting of blocks of ice left by glacier retreat. Remnants of polar material (mapped by *Tanaka and Scott* [4]) also lie within and near the kame-and-kettle–like topography. Previously, we described Olympia Planitia as consisting of remnant Apl covered by sublimation lag now reworked into dunes. Based on subsequent studies of the basal unit, we consider it more likely that Olympia Planitia consists of basal unit material which may itself be a remnant of several stages of polar cap retreat.

Retreat of the polar cap plays a crucial role in its history, because it implies that the north polar cap may not have just appeared in the Late Amazonian but instead may have been influencing the hydrologic and climatic cycles of the planet for much longer and may have waxed and waned with changes in climate.

Possible Scenarios of North Polar Cap History: We have outlined four possible scenarios for north polar cap history [32]. (1) Deposition of the polar cap is a recent event, requiring that climate has only just become favorable for polar cap deposition. We find this case unlikely since a climate largely controlled by orbital parameter variations would not have undergone an overall, large-scale change during the Amazonian other than the smaller scale variations caused by the orbital parameter variations [8]. In addition, in this case, triggers needed to cause melting and retreat would be difficult to achieve in such a short time period. (2) Polar wander [33] has recently brought the caps to their present positions. (3) The polar cap is oscillating, waxing and waning with large changes in orbital parameters, the current polar cap being only the latest manifestation of caps that have come and gone since perhaps the Early Amazonian. Ice deposits may even form at lower latitudes during periods of high obliquity [34]. One possibility is that the major layers of the basal unit each represent a lag left by the retreat of one stage of the polar cap. Since the basal unit is exposed in Chasma Boreale and has been eroded by chasma formation, any melting involved in carving the chasma would have occurred after the last major stage of retreat but may also have occurred during previous stages. *Jakosky et al.* [35] modeled sublimation of the polar cap and found that a pure ice cap of the current Apl thickness could sublimate entirely within 50 x 10^3 yrs. at high obliquities (>45°). (4) The lower layers of the polar cap were deposited in the early Amazonian, and deposition has continued since then; crater counting may reveal only their surface age. In this case, the cap may have undergone more than one stage of partial retreat, and processes such as flow and relaxation [36] may be erasing craters and making the surface appear even younger than it is.

Comparison with the South Polar Cap: The south polar cap shares some characteristics with its northern counterpart. Evidence in the form of esker-like ridges, remnant volatile-rich material, and drainage channels indicate possible retreat of southern polar deposits during the Hesperian [37]. Chasma Australe bears a striking large-scale morphological similarity to Chasma Boreale and thus may also have been formed by melting, yet detailed similarities are few, possibly due to the lack of a southern basal unit and thus lack of a significant source for outflow deposits. *Kolb and Tanaka* [10] cite a dearth of features formed by flow and undisturbed layer sequences in the walls of the chasma as evidence against formation by melting and outflow. Our preliminary searches have shown no evidence for a southern basal unit. Possibly, subsequent stages of growth and retreat of the south polar cap during the Amazonian left no basal unit, though there is evidence for small scale growth and retreat during this time [38]. Perhaps early retreat of the southern deposits left such a thick lag that later retreat was significantly retarded. However, there may exist a much smaller southern basal unit that has not yet been exposed. Further studies should include more comparisons with the south polar deposits so that the ideas developed about the north polar cap can be tested.

References: [1] Soderblom, L. et al. (1973), *JGR* 78, 4197-4210. [2] Cutts, J. (1973) *JGR* 78, 4231-4249. [3] Thomas, P. et al. (1992), in *Mars* (ed. By H. Kieffer et al.), 767-795, U of Ariz. Press, Tucson. [4] Tanaka, K. and D. Scott (1987), *U.S.G.S. Misc. Inv. Ser. Map I-1802-C*. [5] Hoffman, N. (2000), *Icarus* 146, 326-342. [6] Blasius, K. et al. (1982), *Icarus* 50, 140-160. [7] Cutts, J. et al. (1982), *Icarus* 50, 216-244. [8] Laskar, J., et al. (2002), *Nature* 419, 375-377. [9] Tanaka, K. and E. Kolb (2001), *Icarus* 154, 3-21. [10] Kolb, E. and K. Tanaka (2001), *Icarus* 154, 22-39. [11] Pathare, A. and D. Paige, *2nd Int. Conf. Mars Polar Sci. and Exp.*, LPI Contrib. 1057, pg. 79. [12] Hvidberg, C. (2003), *Annal. Glaciol.*, in press. [13] Greve, R. et al. (2003), *Planet. and Space Sci.*, in press. [14] Fisher, D. (2000), *Icarus* 144, 289-294. [15] Clifford, S. (1987), *JGR* 92, 9135-9152. [16] Benito, G. et al. (1997), *Icarus* 129, 528-538. [17] Fishbaugh, K. and J. Head (2002), *JGR* 107, 10.1029/2000JE001351. [18] Zuber, M. et al. (1998), *Science* 282, 2053-2060. [19] Fishbaugh, K. and J. Head (2000), *JGR* 105, 22455-22486. [20] Herkenhoff, K. and J. Plaut (2000), *Icarus* 144, 243-255. [21] Howard, A. et al. (1982), *Icarus* 50, 161-215. [22] Malin, M. and K. Edgett (2001), *JGR* 106, 23429-23570. [23] Milkovich, S. and J. Head (2003), *LPSC* 34, #1342. [24] Byrne, S. and B. Murray (2002), *JGR* 107, 10.1029/2001JE001615. [25] Edgett, K. et al. (2003), *Geomorph.* 52, 289-297. [26] Tanaka, K. et al. (2003), *JGR* 108, 10.1029/2002JE001908. [27] Fishbaugh, K. and J. Head (2003), *6th Mars Conf.*, #3137. [28] Howard, A. (2000), *Icarus* 144, 267-288. [29] Thomas, P. and C. Weitz (1989), *Icarus* 81, 185-215. [30] Fishbaugh, K. and J. Head, *6th Mars Conf.* #3141. [31] Fishbaugh, K. and J. Head (2001), *LPSC* 32, #1426. [32] Fishbaugh, K. and J. Head (2001), *Icarus* 154, 145-161. [33] Schultz, P. and A. Lutz (1988), *Icarus* 73, 91-141. [34] Jakoksy, B. and M. Carr (1985), *Nature* 315, 559-561. [35] Jakosky, B. et al. (1995), *JGR* 100, 1579-1584. [36] Pathare, A. and D. Paige (2003), *LPSC* 34, #2051. [37] Head, J. and S. Pratt, *JGR* 106, 12275-12299. [38] Head, J. (2001), *JGR* 106, 10075-10085.

EXPERIMENTAL INSTRUMENT ON HUNVEYOR FOR COLLECTING BACTERIA BY THEIR ELECTROSTATIC COAGULATION WITH DUST GRAINS (FOELDIX): OBSERVATION OF ELECTROSTATICAL PRECIPITATED COAGULATED UNITS IN A NUTRIENT DETECTOR PATTERN. ***T. Földi[1], Sz. Bérczi[2], E. Palásti[1]*** [1]FOELDIX, H-1117 Budapest, Irinyi József u. 36/b. Hungary, [2]Eötvös University, Department G. Physics, Cosmic Materials Space Res. Gr. H-1117 Budapest, Pázmány Péter s. 1/a, Hungary, (berczi szani@ludens.elte.hu)

ABSTRACT

Electrostatic coagulation properties of dust above planetary surfaces [1-5] were studied by FOELDIX-1 instrument of Hunveyor. We developed FOELDIX-1 by a detector unit in order to observe biomarkers on Mars by collecting dust thrown out from dusty regions. The dust collector experiment [6], with the observation capability of the size dependent dust particles [7], was developed by a nutrient containers which forming a pattern can show various types of bacteria in the inner detector-wall of the FOELDIX-1 instrument [8]. Coagulation of electrostatically charged dust particles, rare H_2O molecules and suggested extremophile bacteria from the dusty Martian surface is transported by our experimental assemblage through the space with electrodes and allows to precipitate in the vicinity of some specially charged electrodes [9]. If living units form a community, a consortia of bacteria and fungla spores with the attached soil then the cryptobiotic crust components of Mars may also be found and distinguished by this measuring technology.

INTRODUCTION

Levitating charged dust particles were measured on Surveyors [1], Apollo's LEAM [2] and their models were shown [3-5], and windstorms on Mars are known since old times and were photographed. We also studied levitating dust particle phenomenon in the experiment of FOELDIX-1 where coagulation of lunar quasiatmospheric dust were modelled [6,8]. We placed the FOELDIX-1 instrument to the Hunveyor electrostatic assemblage. To search the possibility of life on Mars we developed our instrument with bacteria and spora detector unit.

The FOELDIX detector unit consists of spots with nutrient containers. They are placed on the inner wall of the dust collector. They form a coordinate system. (In terrestrial conditions the containers can be replaced with other ones.) In principle the detector unit is similar to the Magnetic Properties Experiment of the Mars Pathfinder, where magnetic materials were fixed on a curtain on the surface of the lander. Magnetic materials were arranged in a characteristic pattern of spots. Magnetic forces glued the magnetized particles on the spots. The repeated dust interaction with this curtain amplified the pattern of the colored dust particles attracted on the spots till the visibility of the pattern. Even by camera observation of the curtain the magnetic spot pattern - with various megnetisation strength of the spots in the curtain magnets - allowed estimation of the magnetisation of the dust particles flown by winds [10].

THE SOIL AND BACTERIA TOGETHER

Extremophile bacteria are among the main constituents of the cryptobiotic crust on the Earth. The FOELDIX instrument has a benefit to colllect the fragments of such living consortia in glued units. This way not only dust but the glued bacteria or other living units (i.e. fungla spores) can be collected into the instruments container. Selected detecting mechanism is necessary to distinguish the various components of the cryptobiotic type living unit fragments of the windblown dry powder material. Therefore a detecting surface with a selective nutrient spot arrangement was constructed for the FEOLDIX. On the Hunveyor we measure the CBC collecting capacity of the instrument in the Great Hungarian Plain where dry alkaline grounds can be found, especially in the Hortobágy.

THE MEASURING DETECTOR ARRANGEMENT

In our measuring detector an inner wall-curtain with various nutrients are fixed in the vicinity of special electrodes. These electrodes allow the coagulated dust and bacteria grains (and other complex particles) to precipitate from the streaming particles in the instrument. The coagulated materials with various bacterial components can grow on the nutrient spots with different effectivity. Repeated interaction of the precipitated dust-and-bacteria coagulates will change the color and extent of the nutrient spot regions and amplifies the pattern of the nutrients till the visibility of the arrangement of spots. Microcamera observation of the detector's spot pattern will show the types of bacteria (or fungla spores) existing inside the coagulated dust particles.

COAGULATION OF PARTICLES CONTAINING DUST+BACTERIA+WATER-MOLECULES

On the inner surface of the electron tube, even in the case of hypervacuum, a monomolecular water molecule layer can be found (Tungsram Factory, [11]). These water molecules are small negative ions and have far longer lifetime then that of the small positive ions [12].

In the vicinity of a dusty planetary surface there exist a space charge of electron cloud. The rare water molecules will act as if they were negatively charged and they preserve their charge. The negatively charged water molecules frequently collide with particles of a positively charged dust cloud producing a complex coagulated particle. This particle is a loose aggregate of ions, has great mass and has lower velocity compared to the small mass particles. While colliding with a negatively charged water molecule the water molecule will attach to the larger one. This process enlarges the complex aggregate larger and larger (we measured coagulation up to 450.000 times mass in the FOELDIX instrument). The living units are embraced and included into this coagulated large particles. Living units are shielded by the dust components from UV and other radiations, and presence of water allows to continue life activity, too.

LOCATION OF PROMISFUL OBSERVATION CHANCES FOR MARTIAN LIVING ORGANISMS: SOUTH POLE

On the MOC MGS images there are promisful regions where to land in order to observe Martian life components of bacteria or fungal spores with dust. In winter these dark dunes are covered with frost. Dark dune spots are formed in

late winter and early spring show a structure on the frost covered surface where the soil material is partially exposed on the surface. This uncovered region is the dark spot itself. In these periods wind blows out the dark dune material from the spots and the ejected dark dust forms a thin layer on the surface of the frost cover.

Dark dune spots (DDSs) were estimated as probable sites for biogenic activity [13-15] and the suggested Martian surface organisms (MSOs) were considered as promisful candidates of the recent life on Mars. If the MSOs exist, then they must be flown out from the dark dune spots during the late winter and early spring period of DDS activity.

PRESENCE OF WATER ON DDS SITES

As we referred earlier the water molecule content of the atmosphere helps the electrostatic coagulation of the dust particles [16]. The Southern Polar region of Mars where the DDS sites were found and studied is therefore promisful source for the FOELDIX experiment because Mars Odyssey also found higher concentration of water in this region [17-19]. Although the 2003/2004 Mars missions will not go to the polar regions, a more detailed imaging may reveal special sites with extensive wind activity in the given late winter early spring period [20, 21].

SUMMARY

The new FOELDIX instrument with the bacteria and spore detector unit is capable to observe various Martian living units coagulated by the instrument and deposited by special electrodes on nutrient spots of the detector. The growing spots can be observed by microcamera units built into the FOELDIX instrument. Such detector can measure not only bacteria but the soil type which is glued with the bacteria. Therefore it is probable that components of the cryptobiotical crust units may be discovered by this measuring technology.

ACKNOWLEDGMENTS

This work was supported by the MÜI-TP-190/2002 and 190/2003 funds of the Hungarian Space Office.

REFERENCES:

[1] Criswell, D. R. (1972): Horizon glow and motion of Lunar dust. *Lunar Science III*. p. 163. LPI, Houston; [2] Rhee, J. W., Berg, O. E., Wolf, H. (1977): Electrostatic dust transport and Apollo 17 LEAM experiment. Space Research XVII. p. 627; [3] Horányi M., Walch, B., Robertson, S. (1998): Electrostatic charging of lunar dust. *LPSC XXIX*. LPI, CD-ROM, #1527; [4] Reid, G. C. (1997): On the influence of electrostatic charging on coagulation of dust and ice particles in the upper mesosphere. *Geophysical Res. Letters*, **24,** No. 9. p. 1095; [5] Sickafoose, A. A., Colwell, J. E., Horányi, M. Robertson, S. (2001): Dust particle charging near surfaces in space. In *LPI XXXII*, #1320, LPI, CD-ROM; [6] T. Földi, R. Ezer, Sz. Bérczi, Sz. Tóth. (1999): Creating Quasi-Spherules from Molecular Material Using Electric Fields (Inverse EGD Effect). *LPSC XXX*. LPI, CD-ROM, #1266.; [7] T. Földi, Sz. Bérczi, E. Palásti (2002): Time Dependent Dust Size Spectrometry (DUSIS) Experiment: Applications in Interplanetary Space and in Planetary Atmospheres/Surfaces on Hunveyor. *Meteoritics & Planetary Science,* **37**, No. 7. Suppl., p. A49.; [8] Földi T., Bérczi Sz., Palásti E. (2001): Water and bacteria transport via electrostatic coagulation and their accumulation at the poles on the dusty planet. *LPSC XXXII*, #1059, LPI, CD-ROM; [9] Földi T., Bérczi Sz. (2001): The source of water molecules in the vicinity of the Moon. *LPSC XXXII*, #1148, LPI, CD-ROM; [10] Hviid, S. F.; Knudsen, J. M.; Madsen, M.B.; Hargraves, R. B. (2000): Spectroscopic Investigation of the Dust Attracted to the Magnetic Properties Experiment on the Mars Pathfinder Lander. *LPSC XXXI*, #1641, LPI, CD-ROM; [11] Bródy I., Palócz K. (1953): Lecture on Techn. Univ. Budapest (personal communication); [12] Israel, H. (1957): *Atmospherische Elektricitet*. Leipzig.; [13] Horváth A., Gánti T., Gesztesi A., Bérczi Sz., Szathmáry E. (2001): Probable evidences of recent biological activity on Mars: Appearance and growing of Dark Dune Spots in the South Polar Region. *LPSC XXXII*, #1543, LPI, CD-ROM; [14] A. Horváth, T. Gánti, Sz. Bérczi, A. Gesztesi, E. Szathmáry (2002): Morphological Analysis of the Dark Dune Spots on Mars: New Aspects in Biological Interpretation. *LPSC XXXIII*, #1108, LPI, CD-ROM; [15] A. Horváth, Sz. Bérczi, T. Gánti, A. Gesztesi, E. Szathmáry (2002): The "Inca City" Region of Mars: Testfield for Dark Dune Spots Origin. *LPSC XXXIII*, #1109, LPI, CD-ROM; [16] T. Földi, Sz. Bérczi (2001): Quasiatmospheric Electrostatic Processes on Dusty Planetary Surfaces: Electrostatic Dust and Water molecule Coagulation and Transport to the Poles. *26th NIPR Symposium Antarctic Meteorites*, Tokyo, p. 21-23.; [17] Mitrofanov, I. G. et al., (2003): Global Distribution of Shallow Water on Mars: Neutron Mapping of Summer-Time Surface by HEND/Odyssey. *LPSC XXXIV,* #1104, LPI, CD-ROM; [18] Kuzmin, R. O.; Mitrofanov, I. G.; Litvak, M. L.; Boynton, W. V.; Saunders, R. S. (2003): Mars: Detaching of the Free Water Signature (FWS) Presence Regions on the Base of HEND/ODYSSEY Data and Their Correlation with Some Permafrost Features from MOC Data. *LPSC XXXIV,* #1369, LPI, CD-ROM; [19] A. Horváth, T. Gánti, Sz. Bérczi, A. Gesztesi, E. Szathmáry (2003): Evidence for Water by Mars Odyssey is Compatible with a Biogenic DDS-Formation Process. *LPSC XXXIV*, #1134, LPI, CD-ROM; [20] Córdoba-Jabonero, C.; Fernández-Remolar, D.; González-Kessler, C.; Lesmes, F.; C. Manrubia, S.; Prieto Ballesteros, O.; Selsis, F.; Bérczi, S.; Gesztesi, A.; Horváth, A. (2003): Analysis of geological features and seasonal processes in the Cavi Novi region of Mars. EGS Conference, Nizza, EAE03-A-13011.; [21] Horvath, A.; Manrubia, S. C.; Ganti, T.; Berczi, S.; Gesztesi, A.; Fernandez-Remolar, D.; Prieto Ballesteros, O.; Szathmary, E. (2003): Proposal for Mars Express: detailed DDS-test in the "Inca City" and "Csontváry" areas. EGS Conference, Nizza, EAE03-A-14142.;

3D SIMULATIONS OF THE EARLY MARS CLIMATE WITH A GENERAL CIRCULATION MODEL. F. Forget[1] , R. M. Haberle[2], F. Montmessin[2], S. Cha[2], E. Marcq[1,2], J. Schaeffer[2], Y. Wanherdrick[1], [1] *Laboratoire de Météorologie Dynamique,IPSL, UPMC BP99, place Jussieu, 75252 Paris cedex 05 (forget@lmd.jussieu.fr)*, [2] *NASA Ames Research Center, Space Science Division, Moffett Field, California*, ..

Introduction

The environmental conditions that existed on Mars during the Noachian period are subject to debate in the community. In any case, there are compelling evidence that these conditions were different than what they became later in the amazonian and possibly the Hesperian periods. Indeed, most of the old cratered terrains are disected by valley networks (thought to have been carved by flowing liquid water), whereas younger surface are almost devoid of such valleys. In addition, there are evidence that the erosion rate was much higher during the early noachian than later [1]. Flowing water is surprising on early Mars because the solar luminosity was significantly lower than today. Even with the thick atmosphere (up to several bars) that is expected to have existed on Mars at the time, simple 1D models based on a purely gaseous atmosphere predicted climate conditions too cold to allow liquid water to flow [2]. On this basis, some authors have suggested that the difference resulted from a stronger geothermalism during that period, and that a warm climate was not necessary to explain the valley network [3]. However, other authors claim that a warm, wet early climate capable of supporting rainfall and surface runoff is the most plausible scenario for explaining the entire suite of geologic features in the Martian cratered highlands [1].

To help understand this key issue in Mars science, it is important to extend the initial climate simulations that concluded that early Mars must have been cold [2,3], since these calculations were performed with very simple 1D models [4]. Such improvements have been performed by several authors, and in particular it has been suggested that the CO_2 ice clouds that must have formed in such an atmosphere could have produced a strong "scattering" greenhouse effect sufficient to warm the planet above the freezing point of water [5]. However, there again, these simulations were performed with simple 1D models, from which it is difficult to predict the environmental conditions.

A Global Climate model for early Mars

To improve our understanding of the early Mars Climate, we have developped a 3D general circulation model similar to the one used on current Earth or Mars to study the details of the climate today. Our first objective is to answer the following questions : how is the Martian climate modified if 1) the surface pressure is increased up to several bars (our baseline: 2 bars) and 2) if the sun luminosity is decreased by 25account the heat possibly released by impacts during short periods, although it may have played a role [6]

For this purpose, we have coupled the Martian General Circulation model developped at LMD [7] with a sophisticated correlated k distribution model developped at NASA Ames Research Center. It is a narrow band model which computes the radiative transfer at both solar and thermal wavelengths (from 0.3 to 250 microns). The correlated-k's for each bands are generated from a line-by-line code using the HITEMP data base from HITRAN. In addition, pressure induced absorption by CO_2 in included using a simple parameterisation from an analytical formula produced by Moore et al. (1971). This is a major source of uncertainty.

In addition to the radiative transfer and to the parameterisation that are usually included in such a climate models (dynamical core to solve the 3D fluid dynamic equations, subgrid scale turbulent and convective mixing, surface heat balance and subsurface heat conduction, etc...), we have included parameterisations to account for the condensation, transport, gravitational sedimentation and radiative effects of the CO_2 ice clouds that readily form in a thick CO_2 atmosphere. model. Using the correlated k distribution model allowed us to compute the complex radiative transfer processes (scattering in the thermal infrared) that cannot usually be accounted for with the usual GCM's wide band model.

Results

Preliminary results obtained assuming a 2 bars atmosphere suggest that, even without taking into account the radiative effect of CO_2 clouds, temperature near or above the freezing point of water may be obtained seasonally in the summer hemisphere. The diurnal amplitude of surface temperature is small, and therefore warm temperatures may last for long periods. CO_2 ice clouds are found to form almost everywhere on the planet in the upper atmosphere above 40 km. Their radiative effect on the climate is very model dependent but, in most cases, should correspond to a warming of the surface.

Ultimately, such a model may enable us to simulate the water cycle by applying parameterisations currently used in Earth models. It will be interesting to investigate wether snow or rain could have occur on such a planet.

Reference

[1] Craddock and Howard, *J.G.R* 107 [2002]
[2] Kasting, *Icarus* **94**,1 (1991)
[3] Squyres and Kasting, *Science* **265**, 744 (1994).
[4] Haberle, *J.G.R* 103, 28467, (1999)
[5] Forget and Pierrehumbert, *Science* 278, 1273 (1997)
[6] Segura et al. *Science* 298, 1977 (2002)
[7] Forget et al. *J.G.R* 104, 24,155 (1999)

BACTERIAL DISTRIBUTION AND PRODUCTION WITHIN LAKE ICE AND GLACIAL ICE ALONG THE FRINGE OF THE ANTARCTIC ICE CAP. C.H. Fritsen[1], J.C. Priscu[2], P.T. Doran[3], [1]Desert Research Institute, Division of Earth and Ecosystem Science, 2215 Raggio Pkwy, Reno, NV 89512 USA, cfritsen@dri.edu, [2]Montana State University, Bozeman, MT 59717 USA, jpriscu@montana.edu., [3]University of Illinois at Chicago, Earth and Environmental Sciences, 845 West Taylor Street (MC186), Chicago, IL 60607 USA, pdoran@uic.edu.

Introduction: Microbial growth within Earth's icy habitats can help define where microbial consortia may survive and function within similar environments on other planets.

Herein, we report on ice properties, bacterial biomass and rates, of bacterial production within perennial lake ice covers and glacial ice environments within the McMurdo Dry Valleys, Antarctica which lie at the border of the Antarctic polar ice cap along the Victoria land coast (Fig. 1).

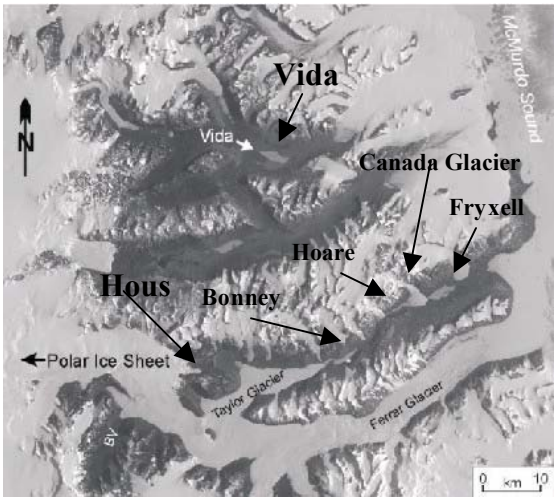

Figure 1: Landsat image of the McMurdo dry valleys region showing location of Lakes Vida, Hoare, Fryxell, Bonney as well as the Taylor, and Canada glaciers. The image is centered at 77.5°S 162°E.

Permanently Ice covered Lakes: Lakes in the McMurdo Dry Valleys of East Antarctica have long been studied as extreme environments and potential analogs of purported Martian lakes of the past [e.g. 1, 2]. Typical, Dry Valley lakes have a 2 to 6 m perennial ice cover overlying 20 to 60 m water columns. These lakes have a range a salinities from fresh to hypersaline, and all allow sufficient sunlight to pass through the ice for photosynthesis to occur in the water column and benthos. Some lakes (e.g. Vida and House) have much thicker ice covers, and it is unknown if the water pockets beneath these ice covers contain viable microbial communities.

Sediment-microbial consortia which are invariably associated with bubble features indicative of liquid water pockets (Fig. 2) are found within the cold ice covers of these lakes [3].

Figure 2. Sediment inclusion from Lake Bonney, with associated arching bubbles indicating the past presence of a melt water pocket. Scale bar is approximately 10 cm.

Glacial Cryoconites: Ablation zones of glaciers also contain sediment inclusions (cryoconites) that harbor microbial consortia [e.g. 4,5]. The sediment-microbiota inclusions are associated with clearer ice created by the melting and refreezing processes which metamorphose the opaque glacial ice by dispersing the small glacial air pockets.

Figure 3: Cryoconite on the Canada Glacier next to author's mitten.

Bacterial numbers: Bacterial cell concentrations range from 4.9e4 to 1.9e7 cells per ml of ice melt water in the lake ice and glacial ice environments. The higher concentrations of bacterial biomass are associated with the ice where sediment inclusions and metamorphosed ice and air inclusions exist (Fig. 3).

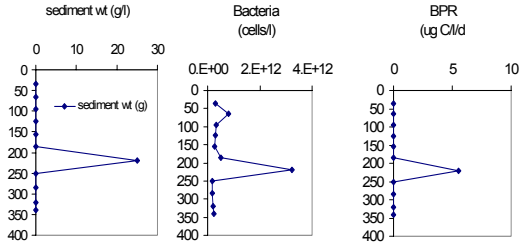

Figure 4. Profiles of sediment content, bacterial cells and bacterial production in the ice cover of Lake Hoare. The coincident peaks of sediment and bacterial abundance and activities are representative of profiles in other lakes as well as enhanced activities in glacial ice with sediment inclusions.

Bacterial Production: Bacterial production rates (BPR) ranged from below levels of detection to 21 ug C l^{-1} d^{-1} in ice melt water. Rates in ice with sediment inclusions averaged ca. 1 ug C l^{-1} d^{-1}.

Rates in ice melt water are not necessarily indicative of *in situ* rates. However, during the summer, these ice habitats experience radiation-induced internal melting [e.g. 6, 7] that creates ice melt water microenvironments. Hence, rates in melt water may be indicative of ice-bound processes. Interestingly, rates of bacterial production relative to measured rates of primary production (PPR) (primarily by cyanobacteria [8]) were comparable (exhibiting rates close to unity) in the samples where BPR and PPR both exceeded 0.1 ug C l^{-1} d^{-1} (Figure 5). Such coincidence in the magnitude of production may be indicative of coupled successional feedback processes that are expected within enclosed systems that reach near steady-state conditions. If these environments do indeed exhibit close coupling we would expect that biomass accrual and biosignature development will be tightly coupled to the ice dynamics that would provide new material to these habitable zones (also see [9]). Recognition of morphological features on the martian polar icescape indicative of such processes may be key to the search for habitable microzones on the Red (and white) Planet.

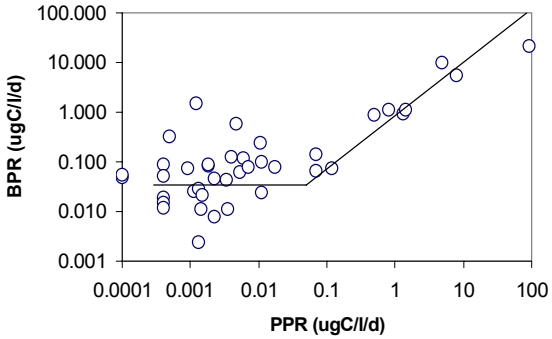

Figure 5: Rates of bacterial production (BPR) relative to primary production (PPR) within lake ice and glacial ice of the McMurdo Dry Valleys.

References: : [1] McKay C. P. et al. (1985) *Nature, 313,* 561-562. [2] Doran P. T. et al. (1998) *JGR, 103(E3),* 28481-28493. [3] Priscu, J.C. et al. (1998) *Science*, 280, 2095-2098. [4] Christner et al. (2002) *Extremophiles*. [5] Muellor D.R. et al. (2001) *Nova Hedwigia*, 123, 173-197. [6] Fritsen, C.H. et al. (1998) *Antarctic Research Series,* 72:269-280. [7] Adams, E.E. et al. (1998) *Antarctic Research Series,* 72:255-268. [8] Fritsen, C.H. et al. (1998) *J. Phycol,* 34, 587-597. [9] Priscu and Christner (In press), *Microbial Diversity and Prospecting*.

ON THE CO_2 HYDRATE PHYSICAL CHEMISTRY AT MARTIAN CONDITIONS. G. Genov and W. F. Kuhs, GZG Abt. Kristallographie, Georg-August-Universität Göttingen, Goldschmidtstr. 1, 37077 Göttingen, Germany (ggenov@gwdg.de; wf.kuhs@geo.uni-goettingen.de)

Introduction: In 1970 Miller and Smythe [1] concluded that the CO_2 hydrate is stable on Mars and that the mixture of pure condensates of CO_2 and H_2O is unstable at the poles. Moreover, some limited kinetic data suggested that the hydrate formation process was fast enough in a meteorological time-scale, which meant, it would lead to a diurnal and annual hydrate cycle. Some authors even put forward the idea that most of the ice in the polar caps was in a hydrate form [2]. Unfortunately, the hydrate and the ice are quite undistinguishable with conventional spectroscopic methods. Moreover, very little is known about the physico-chemical properties of CO_2 hydrates at low temperatures encountered on Mars. We have started to investigate the thermodynamic, physical and kinetic properties of CO_2 hydrate under Martian surface and subsurface p-T conditions.

Possible Importance Of CO_2 Hydrates: Presently is believed that the Martian polar caps consist of water ice, solid CO_2, CO_2 clathrate and dust in unknown proportions, probably different for both caps. The CO_2 clathrate, being the strongest of the three ices could probably affect the rheologic properties of the polar ice layers [3-6] as it was suggested for the north [7] and the south polar caps [8]. If the quantity of the CO_2 hydrate in these regions is large enough it will also influence the process of their basal melting [4, 5]. This is because the hydrates are several times better thermal insulators than water ice and the period needed for establishing a steady-state geothermal gradient in the inner parts of the caps will be much longer.

About The Hydrate Formation: The hydrate formation process is generally believed to start after a certain induction period, needed for some clathrate super nuclei to form. Then the further growth of those nuclei runs in three stages as shown on **Fig. 1**. Guided by the relevance of clathrate hydrate formation from water ice for Mars, a series of kinetic *in-situ* neutron diffraction experiments for CO_2 hydrate formation at higher temperatures were performed. To complement those, a series of pVT formation kinetic experiments were carried out [9]. As a result, applying the model of Salamatin & Kuhs [10, 11], values for the reaction rate coefficients for the different reactions were obtained (**Fig. 2**). A strong bias, of the two points at 272 K and 263 K, from the Arrhenius fit is observed because of the existence of a quasi liquid layer on the surface of the reacting water ice. Thus, two values for the activation energies were obtained – for the high temperature part – 53.5 kJ/mol, and for the low temperature one – 15.5 kJ/mol.

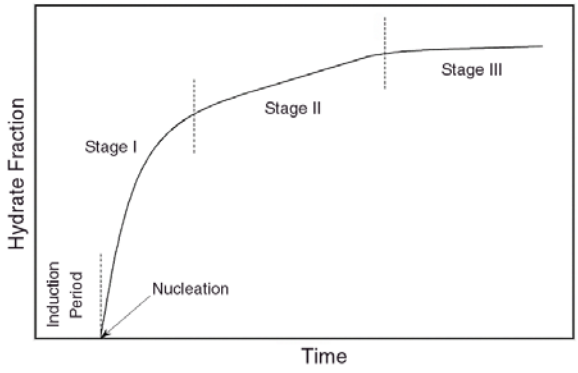

Fig. 1 Stages of the hydrate growth kinetics and induction period.

The delay in formation due to the induction period could be extremely important. Preliminary experiments

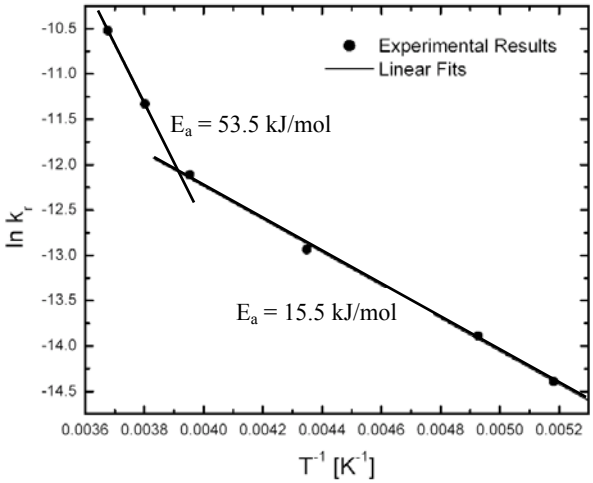

Fig. 2 Plot of the model results for the reaction rate coefficients vs. the temperature.

indicate that the induction period could be several hours up to days at temperatures near 170K and pressures not well exceeding the decomposition pressure of CO_2 hydrate. This may well question the possibility of forming CO_2 hydrate during the Martian night in the diurnal cycle. In our high temperature *in situ* neutron experiments at higher temperatures no induction period was observed within the experimental resolution of 20 s.

Clearly, the induction time depends on temperature and excess pressure and further work is needed to quantify this effect, which is presently under way. Including the effect of induction time in an extended version of the model of Salamatin & Kuhs, we will eventually be in a position to give a realistic prediction for the timescales and kinetics of the hydrate formation at Martian conditions. The kinetics of the growth following the nucleation period is more easily accessible and first estimates will be given in our contribution.

References: [1] Miller S. L. & Smythe W. D. (1970) *Science 170,* 531-533.

[2] Jakosky, B. M. et al. (1995) *J. Geophys. Res., 100, pp. 1579-1584.*

[3] Durham W. B. (1998) *ICMPS, Abstract # 3024*

[4] Kargel J. S. & Tanaka K. L. (2002) *LPS XXXIII, Abstract # 1799*

[5] Kreslavsky M. A. & Head J. W. (2002) *LPS XXXIII Abstract, # 1779*

[6] Kargel J. S. (1998) *ICMPS, Abstract # 3048*

[7] Milkovich S. M. et al. (2002) *LPS XXXIII, Abstract # 171*

[8] Brightwell S. N. et al. (2003) *LPS XXXVI, Abstract # 2077.*

[9] Genov G. & Kuhs W. F. (2003) *VTth ICM, Abstract # 3098.*

[10] Salamatin, A. N. & Kuhs W. F. (2002) *Proc.IV ICGH, pp 766-770*

[11] Staykova, D. K. et al. (2003) *J. Phys. Chem. in press.*

A Radar System for High-Resolution Mapping of Near-Surface Internal Layers in the Polar Ice sheets

S Gogineni, R. Parthasarthy, P. Kanagaratnam, D. Braaten, T. Akins, J Wuite[1] and K. Jezek[1]
The University of Kansas, Radar Systems and Remote Sensing Laboratory
2335 Irving Hill Road, Lawrence, KS 66045-7612, USA
785/864-7734(T) - 785/864-7789 (F) – Gogineni@ittc.ku.edu
[1] BPRC, Ohio State University, Columbus, OH 43210

Accumulation rate is an important variable in determining the mass balance of polar ice sheets. It is currently determined by analyzing ice cores and identifying layers in snow pits, which limits spatial extent over which accumulation rate may be determined. Near-surface internal layers caused by density and conductivity changes can be mapped with a high-resolution radar for estimating accumulation rate. We designed and developed two radars for mapping near-surface internal layers. We developed an airborne radar to operate over the frequency range 600-900 MHz. with a range resolution of about 50 cm to a depth of about 100m. We developed a surface-based system that operates over the frequency range from 500 to 2000 MHz to map layers with 10-cm resolution to a depth of about 100 m. During the 2002 and 2003 field seasons, we collected a large volume of data with the airborne system over the ice sheet in Greenland. We also collected data with the surface-based system at North Greenland Ice Core (NGRIP) drill site in conjunction with detailed in-situ observations from several snow pits and a 15-m firn core. Results from these experiments show that we can map near-surface layers to a depth of atleast 150 m in the dry-snow zone, 120 m in the percolation zone, and 20 m in the melt zone.

In this paper we will discuss the scientific requirements for mapping near-surface internal layers, design considerations and system performance, and present results from airborne and surface-based field experiments. We will also discuss the design of a system for mapping polar-layered deposits in Martian ice caps.

CONSTRAINING THE NATURE AND DISTRIBUTION OF POLAR DEPOSITS ON MARS USING GROUND PENETRATING RADAR. J. A. Grant[1], C. J. Leuschen[2], A. E. Schutz[3], J. Rudy[3], and K. K. Williams[1], [1]Center for Earth and Planetary Studies, National Air and Space Museum, Smithsonian Institution, 6th at Independence SW, Washington, DC, 20560, grantj@nasm.si.edu [2]The Johns Hopkins University, Applied Physics Lab, 11100 Johns Hopkins Road, Laurel, MD, 20723, Carl.Leuschen@jhuapl.edu, [3]Geophysical Surevey Systems, Inc., 13 Klein Drive, North Salem, NH, 03073, alan@geophysical.com.

Introduction: Ground Penetrating Radar (GPR) is capable of addressing a variety of geological problems on the Earth and planets. Terrestrial GPR applications have increased dramatically over the past 30 years and the instrument has become ensconced as an efficient means for non-intrusive definition of radar properties to 10's of meters depth [e.g., 1-3]. Given these capabilities, it is likely that measurements made by a rover-deployed GPR on Mars would help achieve a range of Mars Exploration Program goals including those related to understanding the nature and evolution of polar and near-polar deposits and shallow ground ice [4, 5].

For example, a rover-deployed GPR could penetrate eolian drift or snow masking layered or ground ice-rich units and gullies [6-8] to define the stratigraphy of polar layered deposits [9], the distribution of high latitude ground ice [4, 5], or gully settings. Finally, GPR provides the potential to detect rover hazards (e.g., voids or dust-filled cracks) prior to their engagement. Hence, a GPR could make valuable contributions to rover operations in high latitude settings

Developing a Rover-Deployable GPR for Mars: Careful consideration of the various factors influencing radar performance on Mars instills confidence that a GPR can achieve 10-20 m penetration in high latitude settings [2, 3]. Low ambient temperature and a dry near-surface should reduce electrical losses and mitigate difficulties related to the presence of any fines or salts, thereby enabling radar penetration to on the order of 10 times the wavelength [10]. Magnetic losses may be important in substrates with significant iron-bearing minerals [11, 12], but may be less important in fine-grained, ice-rich polar settings.

Recognizing that a GPR on Mars could constrain stratigraphy and setting to 10-20 m depth is motivation for development of a rover-deployable impulse GPR. Design of our system has focused on development of prototype antennas in parallel with fabrication of a control unit possessing low mass, volume, peak power, and data requirements of 0.5 kg, 3400 cc, 3 W, and ~0.3 MB/day (for 50 meter traverses), respectively. In order to maximize potential penetration and resolution of a Mars GPR, the capability for both high and low frequency investigations has been incorporated. Present designs include a high frequency (600 MHz) bistatic antenna for near-surface high-resolution sounding and a low frequency (100 MHz) monostatic element for deeper probing. Testing of the prototype antennas in terrestrial analog settings confirms the ability to define near-surface stratigraphy that is critical for accurate interpretation of geologic setting (Fig. 1).

Predicting GPR Performance in Polar Settings: Although GPR has been used in high latitude, ice-rich lcoations on the Earth [3], differences in the materials and settings (e.g. dry-ice, more abundant fines) expected in some polar regions of Mars suggest that prediction of GPR performance warrants additional investigation.

A model based on the Finite-Difference Time-Domain (FDTD) method is being used to constrain likely GPR capabilities on Mars and is capable of modeling the complete instrument configuration including antennas, rover, surface roughness, and rocks. The algorithm is a full-wave simulator, is a direct time-domain implementation of Maxwell's curl equations, and can be used to simulate GPR applications as well as process (reverse-time migration) collected data [13]. Simulations highlight the potential value of investing in such models that may enable diagnostic signatures (such as signal attenuation, frequency content, and phase response) to be identified [14], thereby minimizing potential ambiguities associated with detecting an ice rich deposit from radar reflectivity data alone (Fig. 2). Such simulations can facilitate acquisition of dielectric contrasts (from amplitude and phase information), which (with geologic context) could constrain the local geology and setting in polar settings.

Summary: Inclusion of a rover-deployed GPR on a mission targeted to the polar regions of Mars (e.g., 2009 MSL mission) could provide data critical to achieving mission science objectives. Interpretation of GPR data can lead to accurate definition of geologic setting, define the character of stratigraphy associated with layered-terrains, assist in mapping the distribution of near-surface ice, and define the near-surface properties in the vicinity of gullies. As such, data from a GPR could provide context for other rover instruments, and identify sites/samples for in situ analyses.

References: [1] Ulriksen, C.P.F., 1982, Application of Impulse Radar to Civil Engineering: Ph.D. The-

sis, University of Technology, Lund, Sweden, 175p. [2] Grant, J.A., et al. (2003) *J. Geophys. Res*., v. *108*, 10.1029/2002JE001856. [3] Leuschen, C., et al. (2003) *J. Geophys. Res. v. 108*, 10.1029/2002JE001875. [4] Boynton, W. V., et al. (2002), *Science, 297*, 81-85. [5] Feldman, W. C., et al. (2002), *Science, 297*, 75-78, 2002. [6] Christensen, P.R., (1986), J. Geophys. Res., 91, 3533-3545. [7] Ruff, S.W. and Christensen, P.R. (2001) First Landing Site Workshop for the 2003 Mars Exploration Rovers, Ames Research Center, January, 2001. [8] Christensen, P.R., (2003) *Nature, 422*, 45-48. [9] Malin, M. C., and K. S. Edgett (2001), *J. Geophys. Res., 106*, 23,429-23,571. [10] Simpson, R.A., Harmon, et al.(1992), Radar: p. 652-685, in *Mars* (Kieffer, H.H., Jakosky, B.M., Snyder, C.W., and Matthews, M.S., eds.), Univ. Arizona Press, Tucson, AZ, 1498p. [11] Olhoeft, G.R. (1998), Proc. GPR'98, Seventh Int'l Conf. on GPR, University of Kansas, Lawrence, KS, p. 177-182. [12] Paillou, P., et al. (2001), Performances of Ground Penetrating Radars in arid volcanic regions: Consequences for Mars subsurface exploration. [13] Leuschen, C., and R. Plumb, (2001) *IEEE Transactions on Geoscience and Remote Sensing*, *39*, 929-936. [14] Leuschen, C., (2001) *Surface-Penetrating Radar for Mars Exploration*, Ph.D. Dissertation, University of Kansas.

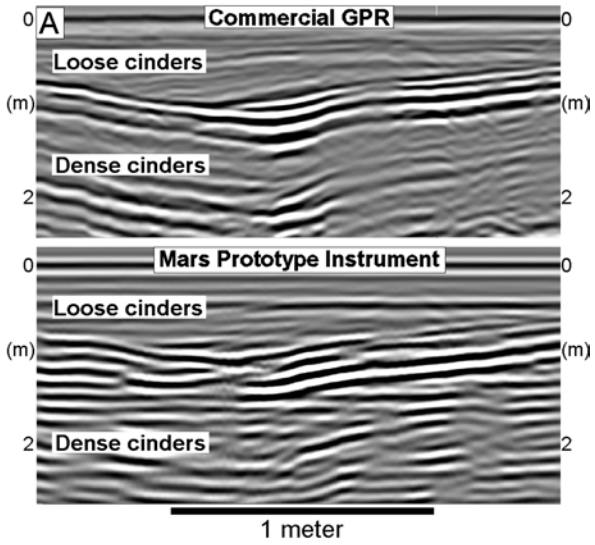

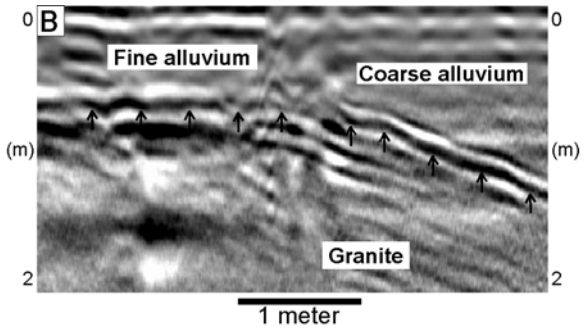

Figure 1. GPR data collected from planetary analog settings using prototype GPR. A) Data from layered volcanic cinders at Sunset Crater, AZ, using commercial 500 MHz antenna (top) and Mars 600 MHz antenna deployed ~15 cm above ground (bottom). B) Data collected using prototype Mars antenna deployed ~15 cm above ground in alluvium over granite bedrock. Arrows show the granite/alluvium contact.

Model: Near-Surface Ice (~2 meters)

top bottom	Lithology	ϕ	*S* ice
0m	atmosphere	100	–
0 m 1.2 m	eolian sediment	50	0
1.2 1.5-2.0	indurated sediment	15	0
1.5-2.0 2.2-2.0	fluvial sediment	30	0
2.2-2.0 6.5-5.5	dirty ice (no rocks)	90	90
6.5-5.5 8.0	non-uniform layered ejecta	10- 20	50

ϕ: porosity (%volume), *S*: saturation

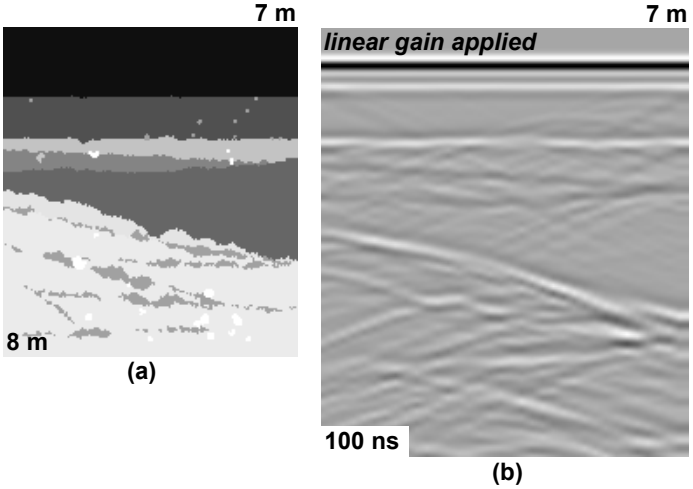

Figure 2 . FDTD simulation of a near-surface ice model. The table describes the stratigraphy, the dielectric distribution is shown in image (a), and the resulting waveforms are in image (b). Numbers in the lower left and upper right of the figure denote simulation depth and distance along the surface, respectively.

INFLUENCE OF ICE RHEOLOGY AND DUST CONTENT ON THE DYNAMICS OF THE NORTH-POLAR CAP OF MARS. Ralf Greve, *Dept. Mechanics, Darmstadt University of Technology, D-64289 Darmstadt, Germany (greve@mechanik.tu-darmstadt.de)*, Rupali A. Mahajan, *Max Planck Institute for Aeronomy, D-37191 Katlenburg-Lindau, Germany*.

Introduction. The Martian poles are both covered by ice caps. The seasonal caps, which can extend down to latitudes of approximately $55^\circ\mathrm{N/S}$, consist of only some ten centimeters of CO_2 snow which sublimes into the atmosphere during the respective summer season. The smaller residual caps poleward of approximately $80^\circ\mathrm{N/S}$ are underlain by massive topographic structures known as the polar layered deposits [11]. The complexes composed of the residual caps and the layered deposits are referred to as the north- and south-polar cap (NPC/SPC), respectively. Owing to the Mars Orbiter Laser Altimeter (MOLA) measurements of the Mars Global Surveyor (MGS) spacecraft, the surface topographies of the NPC and SPC have been mapped very precisely [10,13].

Previous studies [3,4,5] indicate that the NPC is a dynamic ice mass which shows glacial flow of the order of $1\ \mathrm{mm\ a^{-1}}$ at present. Its present topography is the result of the climatic history over the last millions of years, which was probably characterized by climate cycles as a consequence of strong, quasi-periodic variations of the orbital parameters obliquity, eccentricity and precession on time-scales of 10^5–10^6 years [7]. This idea is supported by the light-dark layered deposits of both polar caps indicating a strongly varying dust content of the ice due to varying atmospheric conditions.

In this study, the dynamic and thermodynamic evolution of the NPC will be simulated with the ice-sheet model SICOPOLIS. The boundary conditions of surface accumulation, ablation and temperature are derived directly from the solar-insolation history by applying the Mars Atmosphere-Ice Coupler MAIC developed by Greve et al. [5]. We consider steady-state scenarios under present climate conditions as well as transient scenarios over the last millions of years of climate history. A large uncertainty in model studies of that kind results from the poorly constrained rheological properties of the ice and the unknown dust content. Therefore, we will look systematically into the influence of these two aspects on the evolution of ice topography and glacial flow of the ice body. Some basic considerations for this investigation are given below.

Ice rheology. For terrestrial ice, a well-established non-linear viscous rheology which relates the strain-rate tensor $\boldsymbol{D} = \mathrm{sym\,grad}\,\boldsymbol{v}$ (velocity $\boldsymbol{v}$) to the Cauchy stress deviator $\boldsymbol{t}^{\mathrm{D}}$ is Glen's flow law,

$$\boldsymbol{D} = E A(T') \sigma^{n-1}\, \boldsymbol{t}^{\mathrm{D}}, \tag{1}$$

where $\sigma = [\mathrm{tr}\,(\boldsymbol{t}^{\mathrm{D}})^2/2]^{1/2}$ is the effective shear stress and $n = 3$ the stress exponent. The flow-rate factor depends via the Arrhenius law

$$A(T') = A_0\, e^{-Q/R(T_0+T')} \tag{2}$$

on the temperature relative to the pressure melting point, T', and for $T' \leq -10^\circ C$ suitable values for the constants are $A_0 = 3.985 \times 10^{-13}\ \mathrm{s^{-1}\,Pa^{-3}}$, $Q = 60\ \mathrm{kJ\,mol^{-1}}$ (activation energy), $R = 8.314\ \mathrm{J\,mol^{-1}\,K^{-1}}$ (universal gas constant) and $T_0 = 273.15\ \mathrm{K}$ [9]. The flow-enhancement factor E is equal to unity for pure ice and can deviate from unity due to the softening or stiffening effect of impurities in the ice. A widely used value for terrestrial ice formed during glacial periods is $E = 3$, interpreted as the softening influence of very small amounts of fine dust, approximately $1\ \mathrm{mg\ kg^{-1}}$ with particle sizes of 0.1 to $2\,\mu\mathrm{m}$ [6].

It is not clear whether the flow law (1), which describes the flow mechanism of dislocation creep, is suitable for the low temperatures and low strain rates in the Martian caps. There is strong evidence that other, grain-size-dependent flow mechanisms like grain-boundary sliding become favoured instead [1,2]. These can be described by the flow law

$$\boldsymbol{D} = E A(T') \left(\frac{d_0}{d}\right)^p \sigma^{n-1}\, \boldsymbol{t}^{\mathrm{D}} \tag{3}$$

with the stress exponent $n = 1.8$, the grain size d, the reference grain size $d_0 = 10^{-3}\ \mathrm{m}$ and the grain-size exponent $p = 1.4$. The flow-rate factor $A(T')$ is described by the Arrhenius law (2) with the parameters $A_0 = 9.826 \times 10^{-10}\ \mathrm{s^{-1}\,Pa^{-1.8}}$ and $Q = 49\ \mathrm{kJ\ mol^{-1}}$ [8].

An upper limit for the grain size d can be obtained by assuming that it is a result of normal grain growth only. From a variety of data for terrestrial polar ice masses and theoretical considerations, the growth rate

$$\frac{\mathrm{d}}{\mathrm{d}t}(d^2) = k \tag{4}$$

was derived, where t is the time and $\mathrm{d}/\mathrm{d}t$ is the material time derivative which follows the motion of the ice particles. The growth-rate parameter k depends on the absolute temperature T via the Arrhenius law

$$k(T) = k_0\, e^{-Q_k/RT}, \tag{5}$$

with the activation energy $Q_k = 42.5\ \mathrm{kJ\,mol^{-1}}$ and the constant $k_0 = 9.5\ \mathrm{m^2\,a^{-1}}$ [12]. As an example, for $T = 173\ \mathrm{K}$ this yields a growth rate of $1.40\ \mathrm{mm^2\,Ma^{-1}}$.

Dust content. Satellite imagery shows that parts of the polar caps appear dark, which indicates that they consist of ice with some amount of mixed-in dust. However, for the average volume fraction φ of dust in the ice no quantitative information is available. For modelling studies of the polar caps this is a serious problem because the dust content can affect the ice flow via direct stiffening, an increasing density and a decreasing heat conductivity which leads to basal warming. Therefore, we compute the density, ρ, and heat conductivity, κ, of the ice-dust mixture as volume-fraction-weighed averages of the

values for pure ice and crustal material,

$$\rho = (1-\varphi)\rho_{\rm i} + \varphi\rho_{\rm c}, \quad (6)$$

$$\kappa = (1-\varphi)\kappa_{\rm i} + \varphi\kappa_{\rm c}, \quad (7)$$

with the following parameters: ice density $\rho_{\rm i} = 910\,{\rm kg\,m^{-3}}$, heat conductivity of ice $\kappa_{\rm i} = 9.828\,e^{-0.0057\,T[{\rm K}]}\,{\rm W\,m^{-1}K^{-1}}$, density of crustal material $\rho_{\rm c} = 2900\ {\rm kg\,m^{-3}}$, heat conductivity of crustal material $\kappa_{\rm c} = 2.5\ {\rm W\,m^{-1}\,K^{-1}}$ [4]. Direct stiffening is described by a flow-enhancement factor $E < 1$ based on laboratory measurements of the deformation of ice-dust compounds [1],

$$E = e^{-2\varphi}. \quad (8)$$

This means that a dust content of 10% ($\varphi = 0.1$) leads to an almost 20% stiffer material compared to pure ice.

References. [1] Durham, W. B. (1998). Factors affecting the rheologic properties of Martian polar ice. *First International Conference on Mars Polar Science and Exploration*, LPI Contribution No. 953, pp. 8–9. Lunar and Planetary Institute, Houston. [2] Goldsby, D. L. and D. L. Kohlstedt (1997). Grain boundary sliding in fine-grained ice I. *Scripta Materialia 37* (9), 1399–1406. [3] Greve, R. (2000). Waxing and waning of the perennial north polar H_2O ice cap of Mars over obliquity cycles. *Icarus 144* (2), 419–431. [4] Greve, R., V. Klemann and D. Wolf (2003). Ice flow and isostasy of the north polar cap of Mars. *Planet. Space Sci. 51* (3), 193–204. [5] Greve, R., R. A. Mahajan, J. Segschneider and B. Grieger (2003). Evolution of the north-polar cap of Mars: A modelling study. *Planet. Space Sci.* Submitted. [6] Hammer, C. U., H. B. Clausen, W. Dansgaard, A. Neftel, P. Kristinsdottir and E. Johnson (1985). Continuous impurity analysis along the Dye 3 deep core. In C. C. Langway, H. Oeschger, and W. Dansgaard (Eds.), *Greenland Ice Core: Geophysics, Geochemistry and the Environment*, Geophysical Monographs No. 33, pp. 90–94. American Geophysical Union, Washington DC. [7] Laskar, J., B. Levrard and J. F. Mustard (2002). Orbital forcing of the martian polar layered deposits. *Nature 419* (6905), 375–377. [8] Nye, J. F. (2000). A flow model for the polar caps of Mars. *J. Glaciol. 46* (154), 438–444. [9] Paterson, W. S. B. (1994). *The physics of glaciers*. Third edition. Pergamon Press, Oxford etc. [10] Smith, D. E., and 18 others (1999). The global topography of Mars and implications for surface evolution. *Science 284* (5419), 1495–1503. [11] Thomas, P., S. Squyres, K. Herkenhoff, A. Howard and B. Murray (1992). Polar deposits of Mars. In H. H. Kieffer, B. M. Jakosky, C. W. Snyder, and M. S. Matthews (Eds.), *Mars*, pp. 767–795. University of Arizona Press, Tucson. [12] Thorsteinsson, T. (1996). Textures and fabrics in the GRIP ice core, in relation to climate history and ice deformation. *Reports on Polar Research 205*, 146 pp. Alfred Wegener Institute for Polar and Marine Research, Bremerhaven. [13] Zuber, M. T., and 20 others (1998). Observations of the north polar region of Mars from the Mars Orbiter Laser Altimeter. *Science 282* (5396), 2053–2060.